

signed shields of dense concrete, iron, and lead. In many cases the output data from electronic counters or other apparatus will be transmitted to data-processing electronic computers in the laboratory building, for analysis and recording. A large cryogenics plant for liquefying helium is being built; a separate helium expansion engine will be mounted near the hydrogen bubble chamber, for maintaining low temperature there. Cold helium gas will be used to cool various special targets of hydrogen and deuterium.

Targets located in a straight section can be placed just outside or inside the beam orbit, and the beam can be diverted against the targets by pulsing special magnets or by turning off the radio-frequency acceleration at the peak

of the cycle. High-energy photons are projected forward from such a target in a sharply defined tangential beam. Charged secondary radiations, such as mesons or hyperons produced in a target, can be focused and analyzed magnetically and can pass through other channels in the main shielding wall. Single-beam pulses can be directed at one target (for instance, in a bubble-chamber experiment) and other pulses can be directed at a target serving a different experiment.

In other experiments an emergent beam of 6-Bev electrons will be used. Special magnets located just inside the orbit at chosen straight sections can be pulsed to jolt the electrons out of the orbit into a well-defined emergent beam. This beam will traverse a vacuum pipe

through the shielding wall and will be focused by magnetic lenses onto a target in the experimental hall.

A detailed discussion of the experiments planned is beyond the scope of this account. Scientists from M.I.T. and Harvard, as well as from other nearby universities, are actively engaged in designing experiments that should go far toward exploiting this new energy range in the field of particle physics. No effort is being spared to have the necessary equipment and instruments ready for use when the accelerator is completed.

Notes

1. CEA staff report No. CEA-81 (1 Aug. 1960).
2. Although the average radius of the CEA orbit is 118 feet, the radius of a path segment between the poles of a magnet is shorter—90 feet. In the field-free spaces between magnets the path is straight.

INSTRUMENTS AND TECHNIQUES

Defocusing Images To Increase Resolution

Resolution of two luminous particles is improved by defocusing the microscope or telescope.

Harold Osterberg and Luther W. Smith

Consideration of the distribution of energy density in the diffraction image of two unresolvably small, self-luminous particles led us to expect that a marked increase in the lateral resolving power of a microscope or telescope should occur in appropriately selected out-of-focus image planes. This expectation has been confirmed experimentally. In order to obtain an appreciable advantage, the instrument must be adjusted far out of focus, and thus the appearance of two neighboring concentrations of energy density in the blurred image of two self-luminous particles has, no doubt, either been ignored or considered spurious by many observers.

Particles that are viewed by means of the light that they scatter or cause to fluoresce act, in effect, as self-luminous particles. Particles in a dark-field microscope scatter light into the objective and tend to act almost as though they were

self-luminous. In fact, under certain conditions of illumination, particles appearing against dark backgrounds closely imitate self-luminous particles. These conditions of illumination exist in interference microscopes, in which destructive interference between the direct and the reference beams renders the background practically dark. Conclusions with respect to the out-of-focus states of self-luminous particles apply, therefore, with minor modifications, to suitably illuminated non-self-luminous particles.

The Airy unit is used as the unit of linear measure in the following discussion. The Airy unit r_a is defined by

$$r_a = 0.61 \lambda / \text{N.A.} \quad (1)$$

where λ and N.A. denote wavelength and numerical aperture, respectively. Distance r_a refers to either the object space or the image space, according

to whether N.A. is the numerical aperture of the object space or of the image space of the objective. The numerical aperture with respect to the object space is ordinarily $|M|$ times the numerical aperture with respect to the image space, where M denotes the magnification ratio of the objective.

According to Rayleigh's criterion, two particles are resolved when their separation equals or exceeds one Airy unit. In order that two like particles shall be separated by one Airy unit, their effective radius must not exceed one-half Airy unit. We shall see that it is possible experimentally to resolve two like particles having the separation 0.58 Airy unit. The effective radius of such particles can exceed one-fourth Airy unit only slightly. Such particles are unresolvably small from the viewpoint of diffraction theory.

The family of curves of Fig. 1 shows how the distribution of energy density $I(W)$ in the diffraction image of a single self-luminous particle varies with W for a series of out-of-focus states that are most conveniently and completely specified by the parameter ψ . The variable W is the distance in Airy units from the center of the diffraction image, and

$$\psi = \pi \rho_m^2 z / \lambda \quad (2)$$

where z denotes the out-of-focus distance in the image space and ρ_m denotes the numerical aperture of the objective with respect to its image space. When $\psi = 2\pi$, the eyepiece has been de-

The authors are affiliated with the Research Center, American Optical Co., Southbridge, Mass.

focused by an amount z such that the center of the diffraction image has become dark.

The energy densities $I(W)$ have been normalized so that $I(W)$ equals 1 at $W=0$ for the sharply focused state $\psi=0$. Decisive changes in $I(W)$ occur when ψ exceeds π . The energy content at the diffraction head ($W=0$) diminishes rapidly with ψ , and, as would be expected, the energy content of the diffraction rings increases with ψ . However, the radius of the central bright spot decreases markedly with increasing ψ . If, indeed, one ventures to extend Rayleigh's criterion to the location of the first minimum for the curve $\psi = \pm 3\pi/2$, two particles would be resolved when their separation is only 0.53 Airy unit. This rough prediction is not far from correct.

The curves of Fig. 1 have been computed by an excellent method conceived by Guy Lansraux (1). His notation has been kept, for the convenience of readers who may wish to refer to his article in the *Revue d'optique*.

The graphical method whereby the curves of Fig. 1 have been utilized to obtain information about the combined energy density $I(W)$ in the image of two self-luminous particles is illustrated in Fig. 2 for the case in which the par-

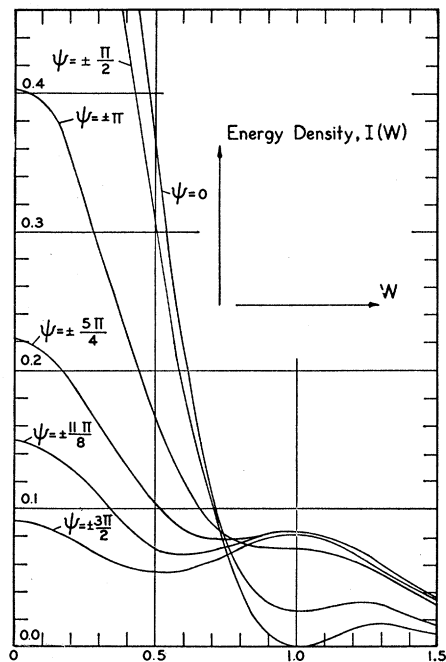


Fig. 1. Plot of the distribution of energy density $I(W)$ against W , the distance in Airy units from the center of the diffraction image of a self-luminous particle for the indicated values of the focal parameter $\psi = \pi \rho_m^2 z / \lambda$. The objective is assumed to be of the idealized Airy type with respect to the sharply focused image plane for which $\psi=0$.

ticles are separated by 0.7 Airy unit. The centers of the geometric images of the particles are located at $W=0$ and $W=0.7$. Because the two self-luminous particles radiate independently, they produce, about the points $W=0$ and $W=0.7$, the independent distributions plotted as the dashed curves A and A' in the sharply focused plane for which $\psi=0$. Addition of the ordinates of curves A and A' amounts to adding the energy densities due to the two particles and produces the corresponding curve A'' for the designated focal state $\psi=0$. Similarly, the combined energy density $I(W)$ of curve B'' for the focal states $\psi = \pm 5\pi/4$ is obtained by adding the ordinates of curves B and B' . In order to form a better comparison of the physical processes involved, the curves A and B have been normalized separately so that $I(W)=1$ at $W=0$. This normalization is equivalent to using a brighter source of light for the focal states $\psi = \pm 5\pi/4$.

Two like particles having the separation 0.7 Airy unit are not resolved in the sharply focused image plane for which $\psi=0$ (curve A'') but may be resolved in the out-of-focus planes for which $\psi = \pm 5\pi/4$ (curve B''). It should be observed that curves A and B practically coincide over a marked distance from the diffraction head at $W=0$ but that curve B has become significantly higher than curve A near $W=0.7$. It is this increase in the energy content of the outer portion of the out-of-focus curves B and B' relative to curves A and A' that accounts for the formation of the maxima near $W=0$ and $W=0.7$ of curve B'' . In this way, the graphical study of a variety of out-of-focus cases showed that the increased energy content of the outer portions of the diffraction image of one particle enhances the probability of resolving two particles.

The curves of Fig. 3 were determined after the manner of curve B'' of Fig. 2, so as to illustrate in a systematic manner how the resolving power for two particles depends upon the focal parameter ψ . Consider, for example, the curve for which $\psi = \pm 3\pi/2$. The centers of the geometrical images of the two particles fall at $W=0$ and $W=0.53$ Airy unit. The corresponding values of energy density are marked P and P' , respectively, with the point P' designated by the circle. The value of the energy density at the midpoint between the geometrical images is marked C and designated by the triangle. Let $I(P)$, $I(P')$ and $I(C)$ denote the

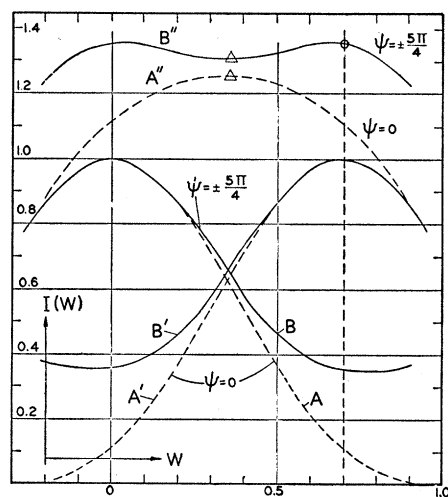


Fig. 2. Plots illustrating how the energy density $I(W)$ in the image of two like particles is determined graphically from the distribution of energy density in the image of one of the particles. The dashed curves pertain to the sharply focused image for which $\psi=0$. The combined energy density in curve A'' is the sum of the ordinates of curves A and A' for two particles separated by 0.7 Airy unit.

energy densities $I(W)$ at the points P , P' , and C , respectively. The separation P to P' has been determined so that, approximately,

$$\frac{I(P) - I(C)}{I(C)} = \frac{I(P') - I(C)}{I(C)} = 0.01 \quad (3)$$

When $\psi = \pm 3\pi/2$, the contrast condition of Eq. 3 is met by choosing the separation P to P' as 0.53 Airy unit.

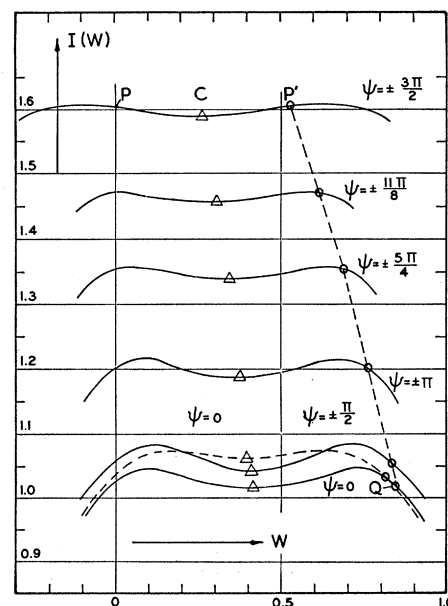


Fig. 3. Plot of distributions of energy density $I(W)$ in the image of two particles for the indicated values of the focal parameter ψ . For each value of ψ the separations P to P' have been determined in accordance with Eq. 3 of the text.

Similarly, all of the curves drawn as solid lines in Fig. 3 have been determined for separations P to P' of the particles in accordance with Eq. 3.

The broken curve belonging to the in-focus state $\psi = 0$ is included for comparison and reference. For this curve the separation of the particles is 0.81 Airy unit—a separation that has been judged resolvable (presumably in the state of sharpest focus) by many observers. Comparison of the curves of Fig. 3 shows that contrast in the image of the two particles equals or exceeds that for the broken curve in the focal state $\psi = 0$. Actual contrast in the diffraction image is usually better than indicated by the fixed value 0.01 of Eq. 3, because the maxima do not ordinarily occur at points P and P' —that is, at the positions of the geometrical images.

Using Eq. 3 as the criterion for resolution, one obtains the broken curve through the points from P' to Q for the corresponding limits of resolution as a function of the focal parameter ψ . For example, with $\psi = \pm 11\pi/8$, this limit of resolution becomes 0.62 Airy unit. Examination of the curve for $\psi = \pm 11\pi/8$ of Fig. 1 shows that the first minimum falls near 0.62 Airy unit, so that one is tempted to invoke Rayleigh's criterion as the practical equivalent of the criterion of Eq. 3. However, this extended notion of Rayleigh's criterion is not in good agreement for ψ values in the range $0 \leq |\psi| \leq \pi$.

The first experimental verification of increased lateral resolution by defocusing was performed with a microscope in the following manner. The substage condenser of a microscope was replaced by an oil immersion objective that served to image the bright disk of a 2-watt zirconium arc with demagnification of about 100. This image was formed in the oil film between two cover plates at the stage and was doubled by placing a Wollaston prism between the arc and the objective. Since neither a polarizer nor an analyzer was employed, the doubled image of the zirconium arc served, in effect, as two self-luminous particles. These "particles" were projected by a $5\times$ objective having a low, fixed numerical aperture determined by the interposition of a suitable diaphragm. The resulting image could be viewed through a focusable eyepiece or could be photographed. Movement of the Wollaston prism along the optic axis of the system permitted continuous adjustment of the separation of these "self-luminous particles" at the rear focal plane of the oil immersion objective,

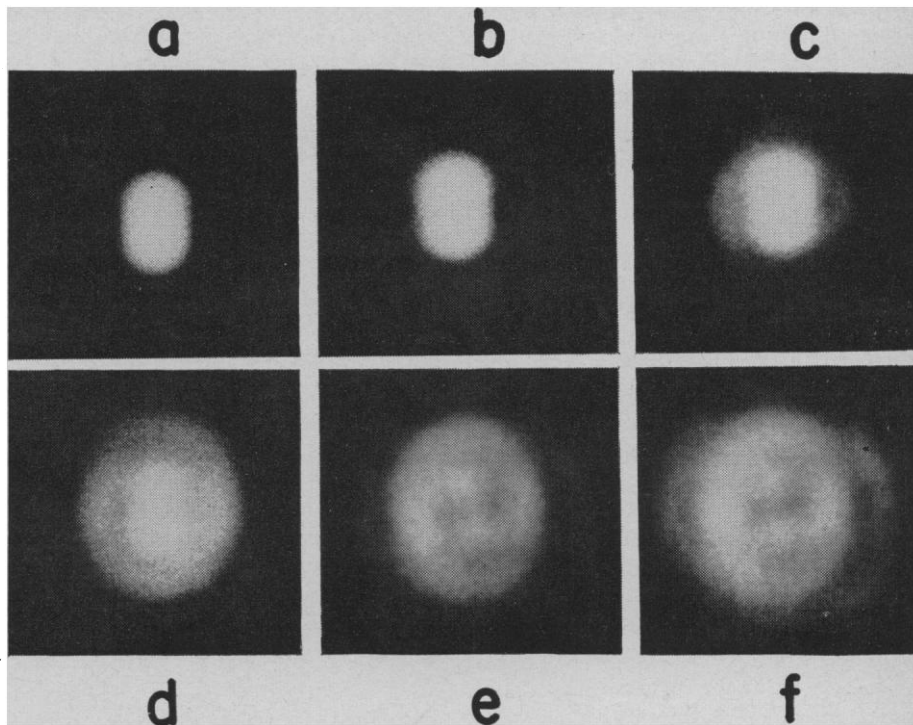


Fig. 4. Photographs illustrating how increased lateral resolution is obtained by defocusing. The distance out of focus is increased progressively from the sharply focused photograph a to the most blurred photograph f . The two particles are resolved in the blurred photographs d , e , and f , but not in the sharply focused image plane of photograph a .

The aperture diaphragm at the $5\times$ objective served also to reduce the numerical aperture of the whole system and thus to avoid aberrations, except for that due to defocus. An interference filter confined the light to a narrow band at 5461 angstroms.

Increased lateral resolving power resulted from moving either the $5\times$ objective or the eyepiece along the optic axis. Motion of the eyepiece is theoretically the preferred method of defocusing, because the numerical aperture of the $5\times$ objective acting as the imaging lens is then undisturbed. In the photographs of Fig. 4 (a to f), the separation of the two particles was fixed at

a value decisively smaller than the limit of resolution in the sharply focused plane (Fig. 4a). In photographs a to f , the amount of defocus is increased progressively up to a point for which $|\psi| < 2\pi$. Although photographs e and f exhibit much blur, the two particles have become well resolved.

More quantitative observations were made by means of the telescopic arrangement shown schematically in Fig. 5. Stopping the N.A. of the telescope objective down to about 0.0063 made it possible to control and measure the separations between pinholes P_1 and P_2 . Distances d_1 and d_2 were about 6 meters and 30 centimeters, respectively.

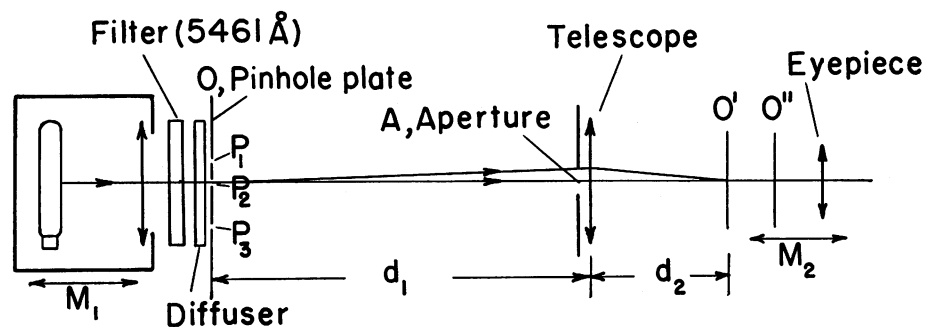


Fig. 5. Diagram of the telescopic arrangement for observing the improvement in lateral resolution of pinholes P_1 and P_2 in out-of-focus image planes. Motion M_1 of the H-4 mercury lamp and pinholes served as fine adjustment of the object distance d_1 . Motion M_2 altered the location of the focal plane O' of the image of O . P_3 is an auxiliary pinhole.

Through motion M_1 of the assembly consisting of the illuminator and pinholes it was possible to adjust the N.A. of the telescope, and hence the separation of the pinholes, in a continuous manner to the desired value (in Airy units). Pinhole P_3 was included as a control and was located many Airy units from the tightly separated pinholes P_1 and P_2 . The image of pinhole P_3 served, for example, to indicate whether or not $|\psi|$ equaled 2π , since the center of the diffraction image of an unresolvably small self-luminous particle becomes dark in the out-of-focus plane associated with $|\psi| = 2\pi$.

Qualitatively, the parfocal images of the double pinholes resembled the parfocal images of the zirconium arc in the microscope experiment. In one quantitative experiment, the separation of particles P_1 and P_2 was adjusted to 0.58

Airy unit, and resolved readily. In this experiment, the two pinholes had a diameter of 0.142 millimeter and a separation, from center to center, of 0.606 millimeter. Distance d_1 (Fig. 5) was 6032 millimeters, and the diameter of aperture A was 3.84 millimeters. Determined attempts to learn how nearly one can approach the limit 0.53 Airy unit of Fig. 3 were not made, since it was felt that a significant determination of an actual limit would require great care.

In an interesting set of preliminary experiments with the microscope arrangement, a marked amount of spherical aberration was added artificially to the $5\times$ objective. It was found that this addition further increased the lateral resolving power, provided that the defocusing was performed on the "cooperative" side of focus.

When pinholes P_1 and P_2 of Fig. 5 were replaced by narrow slits, separations down to 0.73 Airy unit were resolved in the plane of sharpest focus. Defocusing improved lateral resolution of the two slits only slightly. The resolvable separation was decreased only from 0.73 to 0.71 Airy unit. It is noteworthy that the observed in-focus limit of 0.73 Airy unit practically coincides with the physical limit of resolution given by Osterberg (2) for two like slits in an opaque background for the case in which the numerical aperture of the substage condenser of a microscope is set equal to the numerical aperture of the objective.

References

1. G. Lansraux, *Rev. opt.* **26**, 24, Eqs. 26-32 (1947).
2. H. Osterberg, *J. Opt. Soc. Am.* **40**, 295, Fig. 9 (1950).

INSTRUMENTS AND TECHNIQUES

Radio Telemetering from within the Body

Inside information is revealed by tiny transmitters that can be swallowed or implanted in man or animal.

R. Stuart Mackay

It is rather inconvenient to swallow a physician. However, it is quite possible to swallow, or otherwise implant in various body cavities, measuring devices and miniature radio telemetering transmitters which will perform certain of his observation functions. This article attempts to summarize some of these developments and uses as examples some of the methods employed in one laboratory. In the first few sections, some of the physical aspects of these devices are mentioned, and in the last, some examples of application are given for such units. These units have been called endoradiosondes and are so

termed here. They are important in studies of human beings because they leave the subject in a relatively normal physiological state, and they are at least as important in animal studies, where discussion and cooperation are lacking.

In the transmission of internal data there are essentially four possibilities: one can build a passive transmitter or an active transmitter, and one can employ a magnetic dipole or an electric dipole (in the latter, using the conductivity of the body to carry out the signal). All except the passive electric dipole have been demonstrated. There seems no adequate reason to expect the optimum carrier frequency to be the same in any two of the methods. Skin depth gives a rough hint of frequency

but can be misleading; more tests are needed if minimum energy units are desired. In general, these transmitters have been made to work in the frequency range of $\frac{1}{2}$ to 10 megacycles. As in nuclear resonance experiments, passive magnetic transmitters (in which a resonant circuit alone is swallowed) can work either by absorption or by emission, and the best frequency is probably the same in either case. Physiological variables which can cause a change in reactance of a transducer lend themselves to passive as well as active transmission. Almost any system of modulation other than simple amplitude modulation is suitable in any of the methods. Transmitters whose power is induced in the capsule at one frequency or time and reradiated by an active transmitter at another do not involve any different concepts. Non-radio transmission methods, such as monitoring pressure by observing the size of an ingested balloon with ultrasound or x-rays, are not considered here.

Passive Transmission

In passive transmitters the capsule carries no power source but only a resonant circuit whose characteristic frequency is sensed from outside. This frequency is altered by some reactance whose magnitude changes in response to changes in pressure, temperature,

The author is associate research biophysicist and associate clinical professor, School of Optometry, University of California, Berkeley.